Published in final edited form as:
J Card Fail. 2013 January ; 19(1): 60–70. doi:10.1016/j.cardfail.2012.11.003.

Induced overexpression of Na^+/Ca^{2+} exchanger does not aggravate myocardial dysfunction induced by transverse aortic constriction

JuFang Wang, MD[1,*], **Erhe Gao, MD, PhD**[1,*], **Tung O. Chan, PhD**[3], **Xue-Qian Zhang, MD**[1], **Jianliang Song, MD, PhD**[1], **Xiying Shang, MD**[1], **Walter J. Koch, PhD**[1], **Arthur M. Feldman, MD, PhD**[1], and **Joseph Y. Cheung, MD, PhD**[1,2]

[1]Center of Translational Medicine, Temple University School of Medicine, Philadelphia, Pennsylvania 19140

[2]Division of Nephrology, Temple University School of Medicine, Philadelphia, Pennsylvania 19140

[3]Center of Translational Medicine, Jefferson Medical College, Philadelphia, PA 19107

Abstract

Background—Alterations in expression and activity of cardiac Na^+/Ca^{2+} exchanger (NCX1) have been implicated in the pathogenesis of heart failure.

Methods—Using transgenic mice in which expression of rat NCX1 was induced at 5 weeks of age, we performed transverse aortic constriction (TAC) at 8 weeks and examined cardiac and myocyte function at 15–18 weeks post-TAC (age 23–26 weeks).

Results—TAC induced LV and myocyte hypertrophy and increased myocardial fibrosis in both wild-type (WT) and NCX1 overexpressed mice. NCX1 and phosphorylated ryanodine receptor expression was increased by TAC, while sarco(endo)plasmic reticulum Ca^{2+}-ATPase levels were decreased by TAC. Action potential duration was prolonged by TAC, but to a greater extent in NCX1 myocytes. Na^+/Ca^{2+} exchange current was similar between WT-TAC and WT-sham myocytes, but was higher in NCX1-TAC myocytes. Both myocyte contraction and $[Ca^{2+}]_i$ transient amplitudes were reduced in WT-TAC myocytes, but restored to WT-sham levels in NCX1-TAC myocytes. Despite improvement in single myocyte contractility and Ca^{2+} dynamics, induced NCX1 overexpression in TAC animals did not ameliorate LV hypertrophy, increase ejection fraction, or enhance inotropic (maximal first derivative of LV pressure rise, +dP/dt) responses to isoproterenol.

Address Correspondence to: Joseph Y. Cheung, M.D., Ph.D., Center of Translational Medicine, 960-MERB, Temple University School of Medicine, 3500 N. Broad Street, Philadelphia, PA 19140. Tel. 215-707-5418, Fax. 215-707-3989, Joseph.cheung@tuhs.temple.edu.
*J. Wang and E. Gao contributed equally to this work.

Disclosures
No conflict of interest, financial or otherwise, are declared by the authors.

Conclusion—In pressure-overload hypertrophy, induced overexpression of NCX1 corrected myocyte contractile and $[Ca^{2+}]_i$ transient abnormalities but did not aggravate or improve myocardial dysfunction.

Keywords

tet-off; fura-2; in vivo catheterization; intracellular Ca^{2+} regulation

Introduction

The cardiac Na^+/Ca^{2+} exchanger (NCX1) mediates both Ca^{2+} efflux and influx during an action potential (AP) and is therefore intimately involved with regulation of intracellular Na^+ ($[Na^+]_i$) and Ca^{2+} concentrations ($[Ca^{2+}]_i$) during excitation-contraction (EC)(1). Overexpression (2, 3) and downregulation (4) of NCX1 in adult rat left ventricular (LV) myocytes in primary culture result in changes in myocyte contraction and $[Ca^{2+}]_i$ transient amplitudes. Specifically, at low (0.6 mM) extracellular Ca^{2+} concentrations ($[Ca^{2+}]_o$), conditions that favor Ca^{2+} efflux via forward Na^+/Ca^{2+} exchange, overexpression (3) and downregulation (4) of NCX1 resulted in contraction and $[Ca^{2+}]_i$ transient amplitudes that are lower and higher, respectively, when compared to their respective controls. Conversely, at high $[Ca^{2+}]_o$ (5 mM), conditions that favor Ca^{2+} influx via reverse Na^+/Ca^{2+} exchange, contraction and $[Ca^{2+}]_i$ transient amplitudes are higher in NCX1 overexpressed but lower in NCX1 downregulated myocytes, when compared to their respective controls. At physiological $[Ca^{2+}]_o$ (1.8 mM), both contraction and $[Ca^{2+}]_i$ transient amplitudes are similar in NCX1 overexpressed or downregulated myocytes when compared to their respective controls. In the intact heart, homozygous (Hom) but not heterozygous (Het) mice constitutively overexpressing NCX1 exhibit impaired LV fractional shortening (5) while cardiac-specific knockout of NCX1 results in modest diminution of global LV function (6).

We have previously generated a novel transgenic (TG) mouse model in which expression of rat NCX1 TG is under the control of a cardiac-specific promoter driving the expression of a tetracycline transactivator (tTA)(7). When doxycycline (Dox) is removed from the feed at 5 weeks of age, expression of NCX1 TG is induced (Ind), resulting in NCX1 protein levels ~2.5 times that present in wild-type (WT) or non-induced (non-Ind) hearts without changes in expression of other proteins involved in EC coupling. Compared to WT or non-Ind myocytes, Ind myocytes exhibit ~42% higher NCX1 current (I_{NaCa}) amplitude, ~2-fold prolongation of action potential duration, and contraction and $[Ca^{2+}]_i$ transient amplitudes that are lower at 0.6, not different at 1.8, and higher at 5.0 mM $[Ca^{2+}]_o$. Cardiac function, as evaluated by in vivo closed-chest catheterization and echocardiography, is similar among WT, non-Ind and Ind mice. The cardiac phenotype of Ind mice is similar to Het mice constitutively overexpressing NCX1.

Alterations in NCX1 expression and/or activity have been observed in many models of cardiac hypertrophy and heart failure (8). It remains controversial, however, whether increases in NCX1 expression and activity is a beneficial compensatory mechanism in response to contractile dysfunction, or detrimental leading to progressive heart failure. One approach to differentiate whether increased NCX1 expression is “friend or foe” is the ability to “switch on” the expression of NCX1 transgene (TG) concomitantly with the onset of disease state, and evaluate cardiac performance subsequently. In this study, we tested the hypothesis that switching on NCX1 TG expression shortly before transverse aortic constriction (TAC) is beneficial on myocyte and myocardial contractility.

Methods

Generation of inducible NCX1 TG mouse and transverse aortic constriction surgery

Details of inducible NCX1 TG mouse generation and its characterization have been published (7). Briefly, rat NCX1 gene (3) was cloned into a cardiac-specific and inducible controlled vector (TREMHC) composed of a modified mouse α-myosin heavy chain (α-MHC) minimal promoter fused with nucleotide binding sites for tTA (9). NCX1 TG mice engineered on FVB background were crossed with cardiac tTA TG mice in FVB background (MHC-tTA). Littermates that were heterozygous for tTA but negative for NCX1 TG were used as WT controls. In this "tetracycline-off" inducible system, doxycycline (Dox, 300mg/kg mouse diet; Bio-Serv) inhibits tTA transactivation. To induce NCX1 TG expression in adult mice, Dox was removed from the feed at 5 weeks of age. Mice in which the rat NCX1 TG was induced to be expressed are referred to as NCX1 mice throughout this manuscript.

Details of TAC operation have been published (10). Briefly, at 8 weeks of age, mice were anesthetized to a surgical plane with tribromoethanol/amylene hydrate (Avertin; 2.5% wt/vol, 8μl/g ip). Following intubation with a blunt 20-gauge needle and connection to a volume-cycled rodent ventilator (120 breaths/min) on supplemental oxygen (1 L/min), a midline cervical incision was made to expose the trachea and carotid arteries. Aortic constriction was performed by tying a 7–0 nylon suture ligature against a 27-gauge needle. The needle was promptly removed to yield a constriction of approximately 0.4 mm in diameter. Sham operation was identical except that the aorta was not tied. Mice were allowed to recover and studies were performed at 15–18 weeks post-TAC (age 23–26 weeks). Only male mice were used in the studies.

Mice were housed and fed on a 12h:12h light-dark cycle at the Thomas Jefferson University and Temple University Animal Facilities and were supervised by veterinary staff members. Standard care was provided to all mice used for experiments. All protocols applied to the mice in this study were approved and supervised by the Institutional Animal Care and Use Committees at Thomas Jefferson University and Temple University.

Myocardial histopathology

Hearts were harvested from WT-sham, WT-TAC and NCX1-TAC mice (n=3, 4 and 5 for each group, respectively), fixed in freshly prepared formalin in phosphate buffered saline, processed for paraffin sectioning (6 μm thickness), and stained with Masson trichrome. Ten sections were obtained from LV free wall of each mouse. Quantitation of fibrous areas was performed with Sigma Scan Pro5. The ratio of area affected by fibrosis (blue color) to total cardiac area in each section was calculated and expressed as percent fibrosis (11).

Echocardiographic and hemodynamic analyses of cardiac function

Transthoracic two-dimensional echocardiography was performed in anesthetized (2% inhaled isoflurane) mice with a 12-MHz probe as previously described (7, 12–14). LV internal diameters at end-diastole (LVIDD) and end-systole (LVIDS) and ejection fraction (EF) were quantified off-line. For in vivo hemodynamic measurements, a 1.4 French micromanometer-tipped catheter (SPR-671, Millar Instruments, Inc.) was inserted into the right carotid artery and advanced into LV of lightly anesthetized (Avertin) mice with spontaneous respirations and placed on a heated (37°C) pad (7, 12–14). Hemodynamic parameters including heart rate and maximal first time derivative of LV pressure rise (+dP/dt) and fall (−dP/dt) were recorded in closed-chest mode, both at baseline and in response to increasing doses of isoproterenol (Iso; 0.1, 0.5, 1, 5, and 10 ng)(7, 12–14).

Isolation of adult murine cardiac myocytes

Cardiac myocytes were isolated from the LV free wall and septum of WT and NCX1 mice according to the protocol of Zhou et al. (15) and modified by us (7, 12–14, 16, 17). In all experiments, myocytes were used within 2–8 h of isolation.

Myocyte shortening measurements

Myocytes adherent to laminin-coated coverslips were bathed in 0.7 ml of air- and temperature-equilibrated (37°C), HEPES-buffered (20 mM, pH 7.4) medium 199 containing 0.6, 1.8 or 5.0 mM $[Ca^{2+}]_o$. Measurements of myocyte contraction (2 Hz) were performed as previously described (7, 12–14, 16, 17).

$[Ca^{2+}]_i$ transient measurements

Fura–2 loaded (0.67 μM fura–2 AM, 15 min, 37°C) myocytes were field-stimulated to contract (2 Hz, 37°C) in medium 199 containing 0.6, 1.8 or 5.0 mM $[Ca^{2+}]_o$. $[Ca^{2+}]_i$ transient measurements, daily calibration of fura–2 fluorescent signals, and $[Ca^{2+}]_i$ transient analyses were performed as previously described (7, 12–14, 16, 17).

Electrophysiological measurements

I_{NaCa} (7, 13, 14, 16, 18) and action potential (1 Hz)(7, 13, 14, 17) were measured in isolated LV myocytes (30°C) with whole cell patch-clamp. Fire-polished pipettes (tip diameter 4–6 μm) with resistances of 0.8–1.4 MΩ when filled with pipette solutions were used. Compositions of solutions and voltage protocols are given in Figure Legends.

Immunoblotting

Mouse LV homogenates and crude membranes were prepared as previously described (7, 17, 19). For detection of sarco(endo)plasmic reticulum Ca^{2+}-ATPase (SERCA2), α_1- and α_2-subunits of Na^+-K^+-ATPase, and calsequestrin (7.5% SDS-PAGE, reducing conditions with 5% β-mercaptoethanol), Na^+/Ca^{2+} exchanger (7.5% SDS-PAGE, non-reducing conditions with 10 mM N-ethylmaleimide), ryanodine receptor phosphorylated at $serine^{2808}$ (pRyR2)(6% SDS-PAGE, reducing conditions), commercially available antibodies were used as previously described (7, 12, 13, 16, 17, 20). For detection of phospholemman (12% SDS-PAGE, reducing conditions), polyclonal C2 antibody (21) was used. Immunoreactive proteins were detected with enhanced chemiluminescence Western blotting system. Protein band signal intensities were quantitated by scanning autoradiograms of the blot with phosphorimager.

Statistics

All results are expressed as means ± SE. For analysis of I_{NaCa} as a function of group (WT-sham vs. WT-TAC vs. NCX1-TAC) and voltage; in vivo hemodynamic parameters as a function of group and Iso; $[Ca^{2+}]_i$ transient and contraction amplitudes as a function of group and $[Ca^{2+}]_o$; 2-way ANOVA was used. For analysis of echocardiographic parameters, % myocardial fibrosis, action potential parameters and protein abundance, 1-way ANOVA was used. A commercially available software package (JMP version 7, SAS Institute, Cary, NC) was used. In all analyses, $P<0.05$ was taken to be statistically significant.

Results

Effects of TAC ± induced NCX1 TG expression on LV mass, myocyte size, myocardial fibrosis, cardiac contractility and mortality

Fifteen to eighteen weeks post-TAC, LV mass was significantly increased in both WT (~48%; $p<0.0025$) and NCX1 (~64%; $p<0.0006$) when compared to WT-sham mice (Fig. 1). There were no differences in LV mass between WT-TAC and NCX1-TAC animals ($p<0.25$). Whole cell capacitance C_m, an estimate of cell surface membrane area and thus an indicator of cell size, was significantly increased in WT-TAC (~41%; $p<0.0001$) and NCX1-TAC (~31%; $p<0.0001$)(Fig. 1), suggesting most of the LV hypertrophy could be accounted for by increases in myocyte size. In agreement with LV mass, there were no differences in C_m between WT-TAC and NCX1-TAC myocytes ($p<0.22$).

Myocardial histology (Fig. 2) demonstrated significantly ($p<0.008$) increased fibrosis in WT-TAC (0.36 ± 0.08%) and NCX1-TAC (0.30 ± 0.03%) compared to WT-sham (0.06 ± 0.01%) hearts. There were no differences in degree of fibrosis between WT-TAC and NCX1-TAC hearts ($p<0.45$).

There were no significant ($p<0.10$) differences in LVIDD among WT-sham (3.87 ± 0.09 mm; n=5), WT-TAC (4.03 ± 0.12 mm; n=7) and NCX1-TAC (4.22 ± 0.10 mm; n=8) hearts. LVIDS was significantly smaller in WT-sham (2.18 ± 0.11 mm) when compared to either WT-TAC (2.59 ± 0.13 mm; $p<0.045$) or NCX1-TAC (2.80 ± 0.09; $p<0.002$) hearts. There were no differences in LVIDS between WT-TAC and NCX1-TAC hearts ($p<0.25$). EF was significantly reduced in WT-TAC (~12.5%; $p<0.025$) and NCX1-TAC (~16.8%; $p<0.008$) hearts when compared to WT-sham hearts (Fig. 3). EF was not different ($p<0.35$) between WT-TAC and NCX1-TAC hearts.

In vivo hemodynamic measurements corroborated echocardiographic findings in that +dP/dt was significantly lower in WT-TAC (group effect, $p<0.016$) and NCX1-TAC (group effect, $p<0.0001$) mice when compared to WT-sham animals (Fig. 3). There were no differences in +dP/dt between WT-TAC and NCX1-TAC hearts ($p<0.08$). Isoproterenol increased +dP/dt in all 3 groups (Iso effect, $p<0.0001$), but Iso did not affect the magnitude and/or direction of its effects on inotropy across the 3 experimental groups ($p<0.45$, group × Iso interaction effect).

In the present series of experiments, there were 16 WT-sham, 17 WT-TAC and 22 NCX1-TAC mice. There was 1 peri-operative death in WT-TAC group but no mortality was observed in WT-sham and NCX1-TAC groups during the 15–18 weeks post-TAC.

Effects of induced NCX1 TG expression and TAC on I_{NaCa} and action potential

Fifteen to eighteen weeks after TAC, I_{NaCa} was not different ($p<0.32$; group × voltage interaction effect) between WT-sham and WT-TAC myocytes (Fig. 4). Induced overexpression of rat NCX1 TG prior to TAC resulted in ~63% increase in I_{NaCa} ($p<0.0001$; group × voltage interaction effect) in NCX1-TAC compared to either WT-TAC or WT-sham myocytes (Fig. 4).

There were no differences in resting membrane potential ($p<0.45$), action potential amplitude ($p<0.25$) and action potential duration at 50% repolarization (APD_{50})($p<0.35$) among WT-sham, WT-TAC and NCX1-TAC myocytes (Fig. 5). Action potential duration at 90% repolarization (APD_{90}) was significantly ($p<0.0001$) prolonged by TAC in WT myocytes. Induced NCX1 TG expression followed by TAC resulted in additional prolongation of APD_{90} when compared to WT-TAC myocytes ($p<0.01$)(Fig. 5).

Effects of induced NCX1 TG expression and TAC on $[Ca^{2+}]_i$ transients and myocyte contractility

Compared to WT-sham myocytes, systolic $[Ca^{2+}]_i$ was lower in WT-TAC myocytes across the range of $[Ca^{2+}]_o$ examined (Table 1; $p<0.0012$, group effect). Induction of NCX1 TG expression followed by TAC increased systolic $[Ca^{2+}]_i$ so that there was no longer any differences in systolic $[Ca^{2+}]_i$ between WT-sham and NCX1-TAC myocytes ($p<0.07$, group effect). Diastolic $[Ca^{2+}]_i$ was similar among WT-sham, WT-TAC and NCX1-TAC myocytes across the range of $[Ca^{2+}]_o$ examined (Table 1; $p<0.77$, group effect). $[Ca^{2+}]_i$ transient amplitudes were not different between WT-sham and NCX1-TAC ($p<0.17$, group effect) but significantly ($p<0.035$; group effect) lower in WT-TAC myocytes when compared to either WT-sham or NCX1-TAC myocytes (Table 1 and Fig. 6). Half-time of $[Ca^{2+}]_i$ transient decline, an estimate of in situ SR Ca^{2+} uptake (22), was prolonged in WT-TAC myocytes when compared to either WT-sham ($p<0.05$, group effect) or NCX1-TAC myocytes ($p<0.01$, group effect)(Table 1), indicating slower SR Ca^{2+} uptake in WT-TAC myocytes.

Mirroring patterns of $[Ca^{2+}]_i$ transient amplitudes in the 3 groups of myocytes, peak contraction amplitudes were lower in WT-TAC myocytes when compared to WT-sham myocytes ($p<0.001$, group effect)(Fig. 6). The significant group × $[Ca^{2+}]_o$ interaction effects indicated that the inherent differences in myocyte contractility between WT-sham and WT-TAC ($p<0.0009$) and between WT-TAC and NCX1-TAC ($p<0.0007$) myocytes were magnified by changes in $[Ca^{2+}]_o$. There were no differences in myocyte contraction amplitudes between WT-sham and NCX1-TAC myocytes ($p<0.07$, group effect; $p<0.65$, group × $[Ca^{2+}]_o$ interaction effect)(Fig. 6).

Effects of induced NCX1 TG expression and TAC on selected proteins involved in EC coupling

Membrane expression of NCX1 was significantly ($p<0.04$, WT-sham vs. WT-TAC) increased in WT-TAC myocytes (Fig. 7; Table 2), and further elevated in NCX1-TAC myocytes ($p<0.045$; WT-TAC vs. NCX1-TAC). There were no significant differences in membrane expression of α_1-subunit of Na^+-K^+-ATPase among WT-sham, WT-TAC and NCX1-TAC myocytes ($p<0.18$), although expression of α_2-subunit of Na^+-K^+-ATPase was significantly ($p<0.025$) increased in WT-TAC myocytes (Fig. 7; Table 2). Levels of SERCA2 were significantly ($p<0.001$) decreased in WT-TAC and NCX1-TAC when compared to WT-sham myocytes. Levels of ryanodine receptor phosphorylated at serine^{2808} (pRyR2) were higher in WT-TAC when compared to WT-sham ($p<0.0025$) but not NCX1-TAC myocytes ($p<0.2$)(Fig. 7; Table 2). Expression of phospholemman, an endogenous regulator of NCX1 (18), was not different ($p<0.64$) among the 3 groups of myocytes (Fig. 7; Table 2).

Discussion

Transverse aortic constriction in the mouse is an useful model to study pressure-overload hypertrophy. Almost all studies reported LV hypertrophy post-TAC but detecting changes in cardiac function was dependent on the time of measurement and genetic background. For example, Nakamura et al. (23) reported EF declined on Day 1 but returned to normal levels 3 weeks post-TAC in C57BL/6 mice. Marionneau et al. (24) reported that fractional shortening (FS) was similar at 1 week post-TAC in C57BL/6 mice. Zhou et al. (FVB)(10), Roos et al. (C57BL/6 x C3HF1)(5) and Jordan et al. (black Swiss)(25) did not observe any decrement in FS, FS, and EF, respectively, at 3 weeks post-TAC. Funakoshi et al. (FVB)(26) and Hu et al. (C57BL/6)(27) detected no changes in FS and EF at 4 weeks post-TAC. Lu et al. (C57BL/6)(28), Barrick et al. (C57BL/6J)(29) and Hu et al. (C57BL/6)(27)

reported significant decreases in EF at 5, 5 and 6 weeks post-TAC, respectively. From this brief survey, it appears that on average, it takes about 4–5 weeks post-TAC for persistent decrement in myocardial contractility to be manifest. However, genetic background differences have significant impact on the cardiac response to TAC (29) and can account for some of the heterogeneity of results from different laboratories. For example, Barrick et al. reported that C57BL/6J mice suffered a 40% decrement in fractional shortening but 129S1/SvImJ mice had relatively preserved systolic function at 6 weeks post-TAC (29). In myocardial infarction models, outcome of infarct healing in mice is also strongly dependent on genetic background (30). Our current study demonstrated that LV and myocyte hypertrophy, increased myocardial fibrosis, and decreased myocardial performance were observed 15–18 weeks post-TAC in FVB mice.

Alterations in NCX1 expression and/or activity have been observed in many models of cardiac diseases and implicated in the pathogenesis of cardiac dysfunction (8). Focusing on the TAC model of pressure-overload hypertrophy in the mouse, early reports showed 2× increase in NCX1 protein 4–7 weeks post-TAC in FVB mice (31) and 71% increase in NCX1 protein but paradoxical decrease in I_{NaCa} (32 to 62%) 3 weeks post-TAC in C57BL/6 mice (32). Our results were similar in that NCX1 protein levels in WT FVB mice increased by ~40% 15–18 weeks post-TAC but no changes in I_{NaCa} were detected.

Constitutive overexpression of canine NCX1 TG resulted in 2.3-fold and 3.1-fold increase in exchanger activity in Het and Hom transgenic mice (C57BL/6 x C3HF1 background), respectively (5). While WT mice did not suffer significant decreases in FS 3 weeks post-TAC, FS in Het and Hom mice declined by ~39% and ~55% from baseline, respectively (5), suggesting enhanced NCX1 activity aggravated pressure overload hypertropy. Indirect evidence supporting this hypothesis is the observation that inhibiting NCX1 with SEA-0400 improved myocyte contractility at 8 weeks post-TAC in 129Sv/Swiss mice (33). In addition, early studies employing genetic maneuvers to decrease NCX1 expression demonstrated at 3 weeks post-TAC, EF was reduced in WT but not in heterozygous global NCX1 knockout (KO) mice (C57BL/6)(34). The authors suggested that reduction in NCX1 expression resulted in normalization of cardiac function in response to pressure overload. However, it is unusual to detect significant decreases in cardiac function in WT mice at 3–4 weeks post-TAC (5, 10, 25–27). Indeed, more recent studies using an independent heterozygous global NCX1 KO model (~50% NCX1 expression) did not reveal any changes in EF at 3-weeks post-TAC in both WT and NCX1-KO mice (black Swiss)(25). While genetic strain differences may account for the different results, it is also possible that at 3 weeks, TAC did not affect myocardial performance in heterozygous NCX1 KO compared to sham-operated mice. More severe depletion of NCX1 (cardiac-specific NCX1 KO resulting in ~10–20% NCX1 expression) resulted in 100% mortality at 3 weeks post-TAC (25). The literature suggests that increased NCX1 expression may be a maladaptive response to pressure overload, that NCX1 overexpression may lead to worsening myocardial function, and that inhibiting NCX1 function or partially reducing its expression may improve cardiac performance post-TAC. One caveat with these studies is that constitutive overexpression or knockdown of NCX1 resulted in animals being exposed to altered NCX1 activity for a long time before onset of pressure overload, and therefore may not mimic compensatory NCX1 expression changes in response to disease.

The first major finding of the current study is that induction of modest NCX1 overexpression in the heart shortly before TAC did not worsen myocardial dysfunction. This is in contrast to the findings in Het mice constitutively overexpressing canine NCX1 TG in which FS declined by ~39% at 3 weeks post-TAC (5). The reasons for the different results are not intuitively obvious. The level of TG overexpression appears comparable: 2.5-fold increase in NCX1 protein in induced NCX1 hearts (7) vs. 2.34-fold increase in NCX1

activity in sarcolemmal vesicles in Het mice (5), respectively. In addition, modest overexpression of NCX1 TG did not affect baseline cardiac function in both Het and induced NCX1 mice (5, 7). Furthermore, neither induced NCX1 nor Het mice demonstrated any adaptation in expression levels of other calcium handling proteins such as SERCA2, phospholamban, calsequestrin, Na^+-K^+-ATPase and ryanodine receptor (5, 7, 35). Finally, L-type Ca^{2+} current was not affected in either Het or induced NCX1 myocytes (7, 36, 37). A trivial difference is the species origin of NCX1 TG: rat in induced NCX1 vs. dog in Het mice. A second difference is the age at which the animals were subjected to TAC: 8 weeks in the case of induced NCX1 expression (no cardiac hypertrophy)(7) vs. 4 months in the case of Het mice in which cardiac hypertrophy was already evident before TAC (5). A third difference is that Het mice were subjected to increased NCX1 activity for 4 months prior to TAC while induced NCX1 mice had enhanced NCX1 expression and activity for < 3 weeks before TAC. A final difference is that Het mice were of C57BL/6 x C3HF1 background while induced NCX1 mice were of FVB background.

Our results also indicate that increasing NCX1 expression and activity did not ameliorate depressed myocardial performance post-TAC. This is disappointing since the effects of induced NCX1 expression were beneficial at the level of the myocyte. To wit, both $[Ca^{2+}]_i$ transient dynamics and contraction amplitudes in NCX1-TAC myocytes were restored to levels observed in WT-sham myocytes. The inability to translate myocyte improvement into enhanced myocardial performance may be due to LV hypertrophy, subendocardial ischemia due to myocyte:capillary mismatch, alterations in chamber geometry, myocyte loss post-TAC and increased interstitial fibrosis (3- and 5-fold increase at 3 and 5 weeks post-TAC, respectively)(10, 29). Our results indicate that TAC induced similar degrees of LV hypertrophy and myocardial fibrosis in both WT and NCX1 hearts. Based on LVIDD and LVIDS measurements, it appears that there were no gross differences in chamber geometry between WT-TAC and NCX1-TAC hearts. Although we did not perform additional studies to evaluate other possibilities, our results with NCX1-TAC mice clearly demonstrate that depressed myocardial performance can occur without evidence of myocyte contractile dysfunction. In this light, it is interesting to note that normalization of $[Ca^{2+}]_i$ transients and enhancing myocyte shortening by phospholamban ablation did not result in improvement in cardiac function or hypertrophy in two models of heart failure (Gαq overexpression and myosin binding protein mutant MyBP-C_{MUT} expression)(38). In addition, despite clear evidence of depressed contractility in rat hearts evaluated at 3 weeks post-myocardial infarction (MI), $[Ca^{2+}]_i$ transient and contraction amplitudes measured at physiological $[Ca^{2+}]_o$ were similar between sham and post-MI myocytes (39, 40).

SERCA2 expression was depressed at 15–18 weeks post-TAC in both WT and NCX1 myocytes. Our results are different than those of Vinet et al. (B6D2F1/J)(41) and Funakoshi et al. (FVB)(26) who demonstrated no change in SERCA2 at 4 weeks post-TAC. Differences in genetic backgrounds and time post-TAC when measurements were performed may account for the discrepancy in SERCA2 expression. SR Ca^{2+} uptake activity as estimated by $t_{1/2}$ of $[Ca^{2+}]_i$ transient decline, however, was depressed only in WT-TAC but not in NCX1-TAC myocytes. In WT-TAC myocytes, decreased SR Ca^{2+} uptake, elevated phosphorylated RyR2 (and by implication increased SR Ca^{2+} leak)(42), and prolonged APD_{90} (promotes Ca^{2+} efflux via forward Na^+/Ca^{2+} exchange) would all conspire to decrease SR Ca^{2+} content, leading to decreased systolic $[Ca^{2+}]_i$ and reduced $[Ca^{2+}]_i$ transient amplitudes. In NCX1-TAC myocytes, the near normal SR Ca^{2+} uptake activity and phosphorylated RyR2 levels, perhaps with increased Ca^{2+} influx via reverse Na^+/Ca^{2+} exchange during the early part of the action potential, may act synergistically to counter-balance the enhanced Ca^{2+} efflux mediated by increased NCX1 activity during the late phase of the action potential, thereby preserving $[Ca^{2+}]_i$ transients and contraction amplitudes in NCX1-TAC myocytes.

I_{NaCa} was higher and APD_{90} was more prolonged in NCX1-TAC compared to WT-TAC myocytes. APD prolongation was one of the phenotypes in mice with induced NCX1 overexpression, ostensibly due to increased NCX1 activity (7). Despite impressive APD_{90} prolongation, there was no mortality in NCX1 and only 1 peri-operative mortality in WT mice observed during the 15–18 weeks post-TAC, suggesting that arrhythmias and sudden death in models of pressure overload hypertrophy require additional factors besides APD prolongation.

There are caveats to the present study. The first is the report that chronic Dox exposure accelerated LV hypertrophy and progression to heart failure after TAC (41). In that study, Dox (160 mg/kg/d) was administered 1 week before TAC and continued for 1 to 2 months after surgery. Our study design was different in that Dox was only administered during pregnancy and for 5 weeks after birth. Mice with induced NCX1 expression remained Dox-free both 3 weeks before and 15–18 weeks after TAC. The observation that NCX1-TAC myocytes contracted better than WT-TAC myocytes suggested that Dox-exposure pre-TAC was unlikely to adversely affect contractile function. The second is that we use WT rather than mice in which NCX1 TG was not induced (continued Dox exposure) as control. We have previously demonstrated that there were no differences in myocardial and myocyte function between WT and non-induced NCX1 mice (7). More importantly, we would like to avoid the confounding effects of chronic Dox exposure post-TAC on cardiac function (41). The third is that in higher mammals NCX1 facilitates ~28% of Ca^{2+} efflux while it accounts for only 7% of beat-to-beat Ca^{2+} transport in rodents and plays a minor role in relaxation in mouse myocytes (43, 44). Finally, $[Na^+]_i$ in cardiac myocytes is significantly higher in mouse (~12 mM)(45) compared to larger mammals such as rabbits (~7 mM)(45) and this will bias NCX1 less towards the Ca^{2+} efflux and more towards the Ca^{2+} influx mode during an action potential. These last 2 considerations suggest that alterations in cardiac function associated with manipulation of NCX1 expression in mouse cardiac myocytes should be extrapolated to larger mammals with caution.

In summary, induced overexpression of Na^+/Ca^{2+} exchanger did not aggravate pressure overload hypertrophy caused by transverse aortic constriction. Despite restoration of myocyte $[Ca^{2+}]_i$ transients and contractility to normal levels, myocardial performance in pressure overload hypertrophy was not improved by induced overexpression of Na^+/Ca^{2+} exchanger. We conclude that overexpression of Na^+/Ca^{2+} exchanger, by itself alone, is neither a friend nor foe in pressure overload cardiac hypertrophy.

Acknowledgments

This work was supported in part by National Heart, Lung and Blood Institute Grants RO1-HL58672 and RO1-HL74854 (J.Y. Cheung), RO1-HL56205, RO1-HL61690, RO1-HL85503, PO1-HL-75443 and PO1-HL-91799 (W.J. Koch), PO1-HL91799 (Project 2) and the Pennsylvania Research Formulary Fund (A.M. Feldman), and by an American Heart Association Scientist Development Grant F64702 (T.O. Chan).

References

1. Bers DM. Cardiac excitation-contraction coupling. Nature. 2002; 415:198–205. [PubMed: 11805843]
2. Schillinger W, Janssen PM, Emami S, Henderson SA, Ross RS, Teucher N, Zeitz O, Philipson KD, Prestle J, Hasenfuss G. Impaired contractile performance of cultured rabbit ventricular myocytes after adenoviral gene transfer of Na^+-Ca^{2+} exchanger. Circ Res. 2000; 87:581–587. [PubMed: 11009563]
3. Zhang XQ, Song J, Rothblum LI, Lun M, Wang X, Ding F, Dunn J, Lytton J, McDermott PJ, Cheung JY. Overexpression of Na^+/Ca^{2+} exchanger alters contractility and SR Ca^{2+} content in adult rat myocytes. Am J Physiol Heart Circ Physiol. 2001; 281:H2079–2088. [PubMed: 11668069]

4. Tadros GM, Zhang XQ, Song J, Carl LL, Rothblum LI, Tian Q, Dunn J, Lytton J, Cheung JY. Effects of Na^+/Ca^{2+} exchanger downregulation on contractility and $[Ca^{2+}]_i$ transients in adult rat myocytes. Am J Physiol Heart Circ Physiol. 2002; 283:H1616–1626. [PubMed: 12234816]
5. Roos KP, Jordan MC, Fishbein MC, Ritter MR, Friedlander M, Chang HC, Rahgozar P, Han T, Garcia AJ, Maclellan WR, et al. Hypertrophy and heart failure in mice overexpressing the cardiac sodium-calcium exchanger. J Card Fail. 2007; 13:318–329. [PubMed: 17517353]
6. Henderson SA, Goldhaber JI, So JM, Han T, Motter C, Ngo A, Chantawansri C, Ritter MR, Friedlander M, Nicoll DA, et al. Functional adult myocardium in the absence of Na^+-Ca^{2+} exchange: cardiac-specific knockout of NCX1. Circ Res. 2004; 95:604–611. [PubMed: 15308581]
7. Wang J, Chan TO, Zhang XQ, Gao E, Song J, Koch WJ, Feldman AM, Cheung JY. Induced overexpression of Na^+/Ca^{2+} exchanger transgene: Altered myocyte contractility, $[Ca^{2+}]_i$ transients, SR Ca^{2+} contents and action potential duration. Am J Physiol Heart Circ Physiol. 2009; 297:H590–H601. [PubMed: 19525383]
8. Sipido K, Volders P, Vos M, Verdonck F. Altered Na/Ca exchange activity in cardiac hypertrophy and heart failure: a new target for therapy? Cardiovasc Res. 2002; 53:782–805. [PubMed: 11922890]
9. Sanbe A, Gulick J, Hanks MC, Liang Q, Osinska H, Robbins J. Reengineering inducible cardiac-specific transgenesis with an attenuated myosin heavy chain promoter. Circ Res. 2003; 92:609–616. [PubMed: 12623879]
10. Zhou J, Lal H, Chen X, Shang X, Song J, Li Y, Kerkela R, Doble BW, MacAulay K, DeCaul M, et al. GSK-3α directly regulates β-adrenergic signaling and the response of the heart to hemodynamic stress in mice. J Clin Invest. 2010; 120:2280–2291. [PubMed: 20516643]
11. Heineke J, Wollert KC, Osinska H, Sargent MA, York AJ, Robbins J, Molkentin JD. Calcineurin protects the heart in a murine model of dilated cardiomyopathy. J Mol Cell Cardiol. 2010; 48:1080–1087. [PubMed: 19854199]
12. Wang J, Gao E, Song J, Zhang XQ, Li J, Koch WJ, Tucker AL, Philipson KD, Chan TO, Feldman AM, et al. Phospholemman and β-adrenergic stimulation in the heart. Am J Physiol Heart Circ Physiol. 2010; 298:H807–H815. [PubMed: 20008271]
13. Wang J, Gao E, Rabinowitz J, Song J, Zhang XQ, Koch WJ, Tucker AL, Chan TO, Feldman AM, Cheung JY. Regulation of in vivo cardiac contractility by phospholemman: role of Na^+/Ca^{2+} exchange. Am J Physiol Heart Circ Physiol. 2011; 300:H859–868. [PubMed: 21193587]
14. Song J, Gao E, Wang J, Zhang XQ, Chan TO, Koch WJ, Shang X, Joseph JI, Peterson BZ, Feldman AM, et al. Constitutive overexpression of phospholemman S68E mutant results in arrhythmias, early mortality and heart failure: Potenial involvement of Na^+/Ca^{2+} exchanger. Am J Physiol Heart Circ Physiol. 2012; 302:H770–H781. [PubMed: 22081699]
15. Zhou YY, Wang SQ, Zhu WZ, Chruscinski A, Kobilka BK, Ziman B, Wang S, Lakatta EG, Cheng H, Xiao RP. Culture and adenoviral infection of adult mouse cardiac myocytes: methods for cellular genetic physiology. Am J Physiol Heart Circ Physiol. 2000; 279:H429–436. [PubMed: 10899083]
16. Song J, Zhang XQ, Wang J, Cheskis E, Chan TO, Feldman AM, Tucker AL, Cheung JY. Regulation of cardiac myocyte contractility by phospholemman: Na^+/Ca^{2+} exchange vs. Na^+-K^+-ATPase. Am J Physiol Heart Circ Physiol. 2008; 295:H1615–H1625. [PubMed: 18708446]
17. Tucker AL, Song J, Zhang XQ, Wang J, Ahlers BA, Carl LL, Mounsey JP, Moorman JR, Rothblum LI, Cheung JY. Altered contractility and $[Ca^{2+}]_i$ homeostasis in phospholemman-deficient murine myocytes: Role of Na^+/Ca^{2+} exchange. Am J Physiol Heart Circ Physiol. 2006; 291:H2199–H2209. [PubMed: 16751288]
18. Zhang XQ, Ahlers BA, Tucker AL, Song J, Wang J, Moorman JR, Mounsey JP, Carl LL, Rothblum LI, Cheung JY. Phospholemman inhibition of the cardiac Na^+/Ca^{2+} exchanger. Role of phosphorylation. J Biol Chem. 2006; 281:7784–7792. [PubMed: 16434394]
19. Song J, Zhang XQ, Ahlers BA, Carl LL, Wang J, Rothblum LI, Stahl RC, Mounsey JP, Tucker AL, Moorman JR, et al. $Serine^{68}$ of phospholemman is critical in modulation of contractility, $[Ca^{2+}]_i$ transients, and Na^+/Ca^{2+} exchange in adult rat cardiac myocytes. Am J Physiol Heart Circ Physiol. 2005; 288:H2342–2354. [PubMed: 15653756]

20. Wang X, Gao G, Guo K, Yarotskyy V, Huang C, Elmslie KS, Peterson BZ. Phospholemman modulates the gating of cardiac L-type calcium channels. Biophys J. 2010; 98:1149–1159. [PubMed: 20371314]
21. Song J, Zhang X, Carl L, Qureshi A, Rothblum L, Cheung J. Overexpression of phospholemman alter contractility and $[Ca^{2+}]_i$ transients in adult rat myocytes. Am J Physiol Heart Circ Physiol. 2002; 283:H576–H583. [PubMed: 12124204]
22. Zhang XQ, Ng YC, Moore RL, Musch TI, Cheung JY. In situ SR function in postinfarction myocytes. J Appl Physiol. 1999; 87:2143–2150. [PubMed: 10601161]
23. Nakamura A, Rokosh DG, Paccanaro M, Yee RR, Simpson PC, Grossman W, Foster E. LV systolic performance improves with development of hypertrophy after transverse aortic constriction in mice. Am J Physiol Heart Circ Physiol. 2001; 281:H1104–1112. [PubMed: 11514276]
24. Marionneau C, Brunet S, Flagg TP, Pilgram TK, Demolombe S, Nerbonne JM. Distinct cellular and molecular mechanisms underlie functional remodeling of repolarizing K^+ currents with left ventricular hypertrophy. Circ Res. 2008; 102:1406–1415. [PubMed: 18451341]
25. Jordan MC, Henderson SA, Han T, Fishbein MC, Philipson KD, Roos KP. Myocardial function with reduced expression of the sodium-calcium exchanger. J Card Fail. 2010; 16:786–796. [PubMed: 20797603]
26. Funakoshi H, Chan TO, Good JC, Libonati JR, Piuhola J, Chen X, MacDonnell SM, Lee LL, Herrmann DE, Zhang J, et al. Regulated overexpression of the A_1-adenosine receptor in mice results in adverse but reversible changes in cardiac morphology and function. Circulation. 2006; 114:2240–2250. [PubMed: 17088462]
27. Hu X, Xu X, Huang Y, Fassett J, Flagg TP, Zhang Y, Nichols CG, Bache RJ, Chen Y. Disruption of sarcolemmal ATP-sensitive potassium channel activity impairs the cardiac response to systolic overload. Circ Res. 2008; 103:1009–1017. [PubMed: 18802029]
28. Lu Z, Fassett J, Xu X, Hu X, Zhu G, French J, Zhang P, Schnermann J, Bache RJ, Chen Y. Adenosine A_3 receptor deficiency exerts unanticipated protective effects on the pressure-overloaded left ventricle. Circulation. 2008; 118:1713–1721. [PubMed: 18838560]
29. Barrick CJ, Rojas M, Schoonhoven R, Smyth SS, Threadgill DW. Cardiac response to pressure overload in 129S1/SvImJ and C57BL/6J mice: temporal- and background-dependent development of concentric left ventricular hypertrophy. Am J Physiol Heart Circ Physiol. 2007; 292:H2119–2130. [PubMed: 17172276]
30. van den Borne SW, van de Schans VA, Strzelecka AE, Vervoort-Peters HT, Lijnen PM, Cleutjens JP, Smits JF, Daemen MJ, Janssen BJ, Blankesteijn WM. Mouse strain determines the outcome of wound healing after myocardial infarction. Cardiovasc Res. 2009; 84:273–282. [PubMed: 19542177]
31. Ito K, Yan X, Tajima M, Su Z, Barry WH, Lorell BH. Contractile reserve and intracellular calcium regulation in mouse myocytes from normal and hypertrophied failing hearts. Circ Res. 2000; 87:588–595. [PubMed: 11009564]
32. Wang Z, Nolan B, Kutschke W, Hill JA. Na^+-Ca^{2+} exchanger remodeling in pressure overload cardiac hypertrophy. J Biol Chem. 2001; 276:17706–17711. [PubMed: 11279089]
33. Ozdemir S, Bito V, Holemans P, Vinet L, Mercadier JJ, Varro A, Sipido KR. Pharmacological inhibition of Na/Ca exchange results in increased cellular Ca^{2+} load attributable to the predominance of forward mode block. Circ Res. 2008; 102:1398–1405. [PubMed: 18451338]
34. Takimoto E, Yao A, Toko H, Takano H, Shimoyama M, Sonoda M, Wakimoto K, Takahashi T, Akazawa H, Mizukami M, et al. Sodium calcium exchanger plays a key role in alteration of cardiac function in response to pressure overload. Faseb J. 2002; 16:373–378. [PubMed: 11874986]
35. Terracciano C, DeSouza A, Philipson KD, MacLeod K. Na^+-Ca^{2+} exchange and sarcoplasmic reticular Ca^{2+} regulation in ventricular myocytes from transgenic mice overexpression the Na^+-Ca^{2+} exchanger. J Physiol (Lond). 1998; 512:651–667. [PubMed: 9769411]
36. Yao A, Su Z, Nonaka A, Zubair I, Lu L, Philipson KD, Bridge JH, Barry WH. Effects of overexpression of the Na^+-Ca^{2+} exchanger on $[Ca^{2+}]_i$ transients in murine ventricular myocytes. Circ Res. 1998; 82:657–665. [PubMed: 9546374]

37. Adachi-Akahane S, Lu L, Li Z, Frank JS, Philipson KD, Morad M. Calcium signaling in transgenic mice overexpressing cardiac Na^+-Ca^{2+} exchanger. J Gen Physiol. 1997; 109:717–729. [PubMed: 9222898]
38. Song Q, Schmidt AG, Hahn HS, Carr AN, Frank B, Pater L, Gerst M, Young K, Hoit BD, McConnell BK, et al. Rescue of cardiomyocyte dysfunction by phospholamban ablation does not prevent ventricular failure in genetic hypertrophy. J Clin Invest. 2003; 111:859–867. [PubMed: 12639992]
39. Anand I, Liu D, Chugh S, Prahash A, Gupta S, John R, Popescu F, Chandrashekhar Y. Isolated myocyte contractile function is normal in post infarct remodeled rat heart with systolic dysfunction. Circulation. 1997; 96:3974–3984. [PubMed: 9403622]
40. Cheung JY, Musch TI, Misawa H, Semanchick A, Elensky M, Yelamarty RV, Moore RL. Impaired cardiac function in rats with healed myocardial infarction: cellular vs. myocardial mechanisms. Am J Physiol Cell Physiol. 1994; 266:C29–C36.
41. Vinet L, Rouet-Benzineb P, Marniquet X, Pellegrin N, Mangin L, Louedec L, Samuel JL, Mercadier JJ. Chronic doxycycline exposure accelerates left ventricular hypertrophy and progression to heart failure in mice after thoracic aorta constriction. Am J Physiol Heart Circ Physiol. 2008; 295:H352–360. [PubMed: 18487442]
42. Marx SO, Reiken S, Hisamatsu Y, Jayaraman T, Burkhoff D, Rosemblit N, Marks AR. PKA phosphorylation dissociates FKBP12.6 from the calcium release channel (ryanodine receptor): defective regulation in failing hearts. Cell. 2000; 101:365–376. [PubMed: 10830164]
43. Bassani JW, Bassani RA, Bers DM. Relaxation in rabbit and rat cardiac cells: species-dependent differences in cellular mechanisms. J Physiol. 1994; 476:279–293. [PubMed: 8046643]
44. Bers DM. Cardiac Na/Ca exchange function in rabbit, mouse and man: what's the difference. J Mol Cell Cardiol. 2002; 34:369–373. [PubMed: 11991726]
45. Despa S, Islam MA, Pogwizd SM, Bers DM. Intracellular [Na^+] and Na^+ pump rate in rat and rabbit ventricular myocytes. J Physiol. 2002; 539:133–143. [PubMed: 11850507]
46. Zhang XQ, Qureshi A, Song J, Carl LL, Tian Q, Stahl RC, Carey DJ, Rothblum LI, Cheung JY. Phospholemman modulates Na^+/Ca^{2+} exchange in adult rat cardiac myocytes. Am J Physiol Heart Circ Physiol. 2003; 284:H225–233. [PubMed: 12388273]
47. Zhang XQ, Zhang LQ, Palmer BM, Ng YC, Musch TI, Moore RL, Cheung JY. Sprint training shortens prolonged action potential duration in postinfarction rat myocyte: mechanisms. J Appl Physiol. 2001; 90:1720–1728. [PubMed: 11299261]

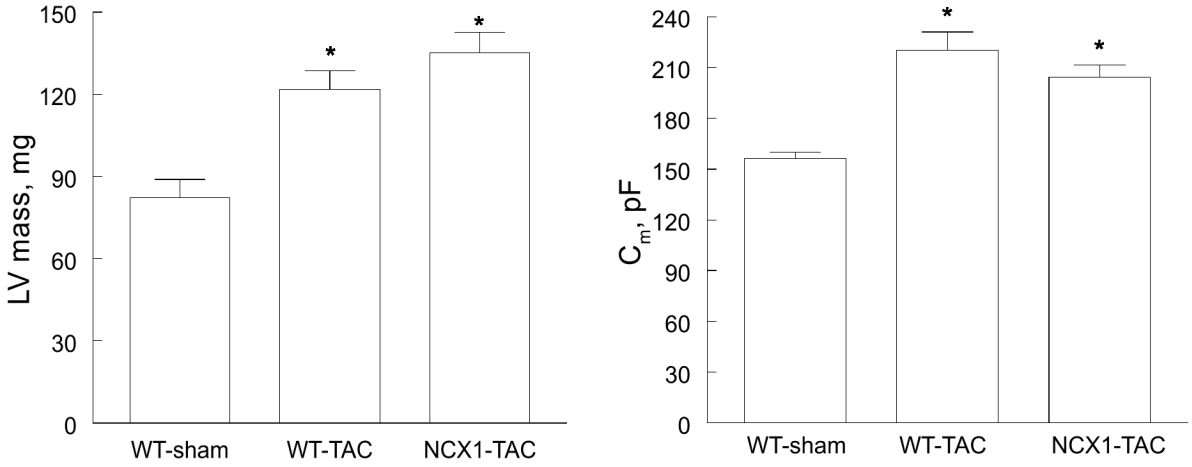

Figure 1. Effects of induced overexpression of Na^+/Ca^{2+} exchanger (NCX1) and transverse aortic constriction (TAC) on left ventricular (LV) mass and whole cell capacitance (C_m)

Expression of rat NCX1 transgene was induced by leaving doxycycline (300mg/kg) off the diet at week 5 of age (Methods). TAC or sham operation was performed at week 8 of age and mice were studied at 15–18 weeks post-TAC (23–26 weeks of age). Left: LV mass of 5 WT-sham, 7 WT-TAC and 8 NCX1-TAC mice. Right: C_m of 21 WT-sham, 15 WT-TAC and 20 NCX1-TAC myocytes. *$p<0.0025$, NCX1-TAC or WT-TAC vs. WT-sham.

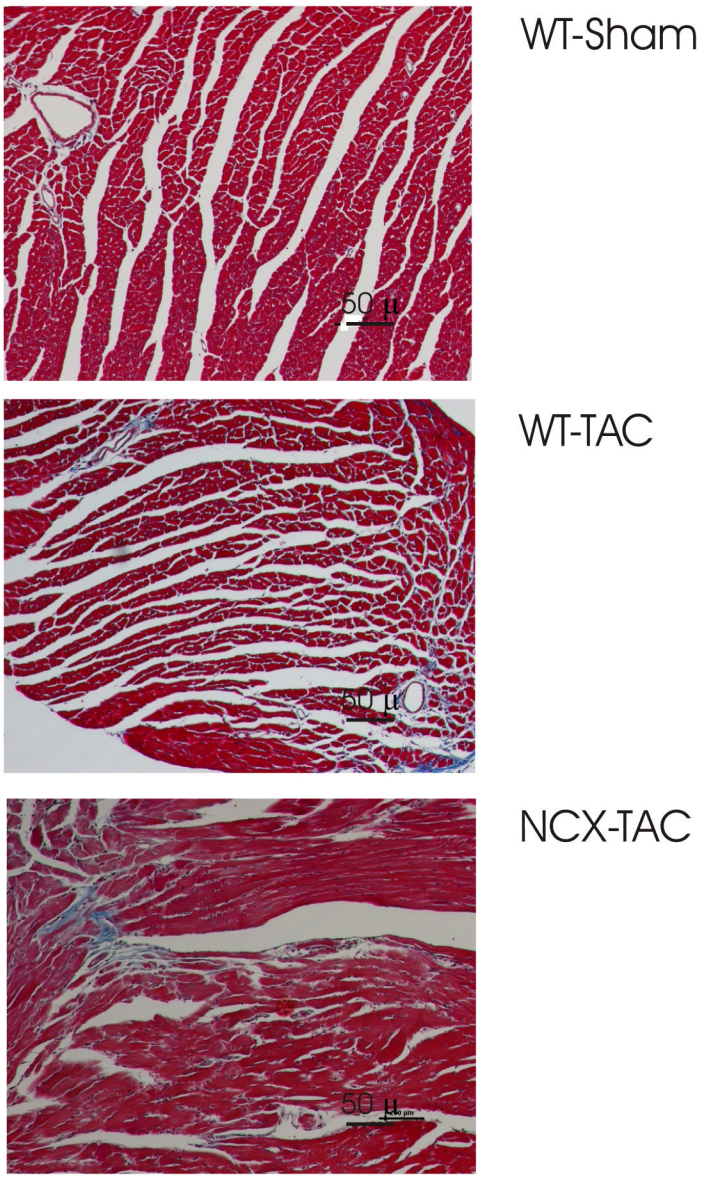

Figure 2. Effects of TAC on myocardial histology in WT and induced NCX1 hearts

Hearts from 15–18 weeks post-TAC or sham-operated mice were stained with Masson trichrome. Representative images from WT-sham (top), WT-TAC (middle) and NCX1-TAC (bottom) hearts are shown. Data are summarized in Results.

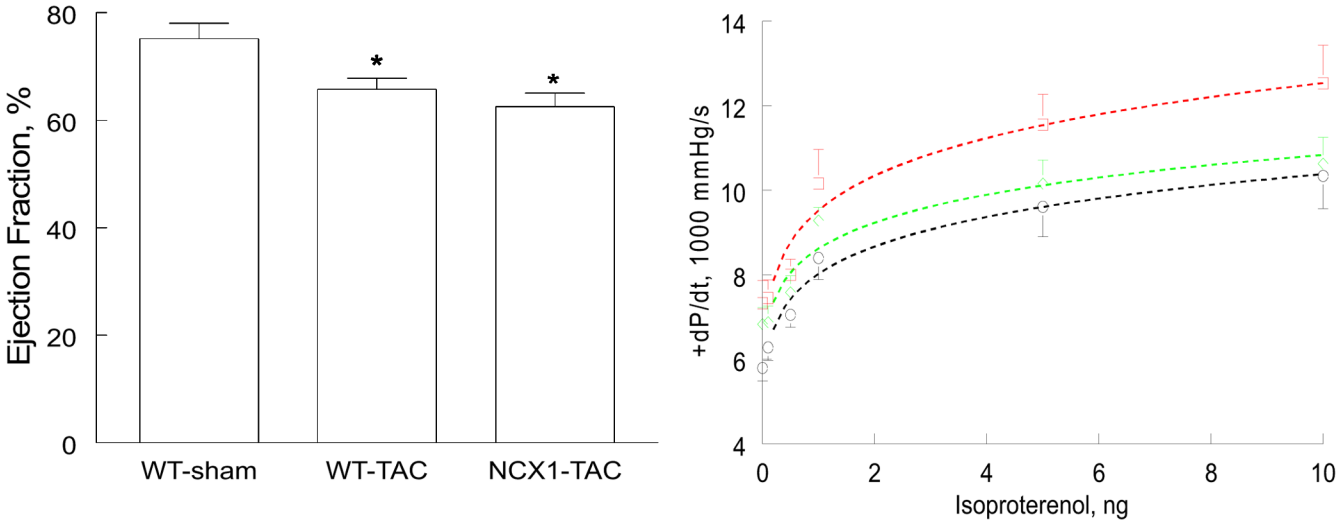

Figure 3. Effects of induced overexpression of Na^+/Ca^{2+} exchanger (NCX1) and transverse aortic constriction (TAC) on left ventricular (LV) ejection fraction (EF) and maximal first time derivative of LV pressure rise (+dP/dt)

Left: LVEF was determined by echocardiography in 5 WT-sham, 7 WT-TAC and 8 NCX1-TAC mice. *p<0.025, WT-sham vs. WT-TAC or NCX1-TAC. Right: In vivo catheterization was performed in anesthetized mice (Methods) and LV pressures and heart rate were continuously monitored, both at baseline and at increasing doses of isoproterenol (Iso). Averaged +dP/dt achieved with each dose of Iso in 5 WT-sham (□), 5 WT-TAC (◆) and 10 NCX1-TAC (○) mice are shown. Error bars are not shown if they fall within the boundaries of the symbol.

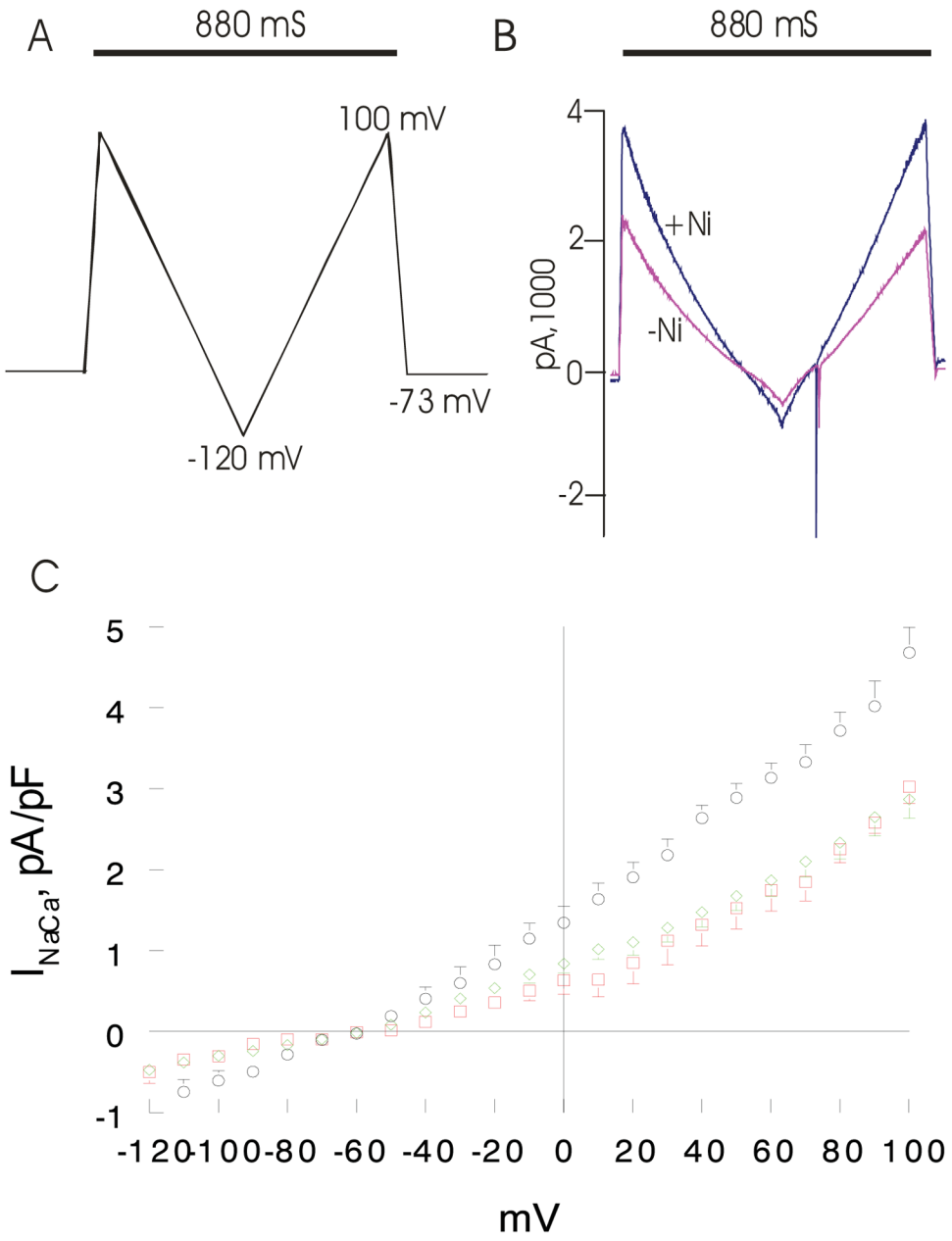

Figure 4. Effects of induced overexpression of Na^+/Ca^{2+} exchanger (NCX1) and transverse aortic constriction (TAC) on NCX1 current (I_{NaCa})

Pipette solution contained (in mM) 100 Cs^+ glutamate, 7.25 NaCl, 1 $MgCl_2$, 20 HEPES, 2.5 Na_2ATP, 10 EGTA and 6 $CaCl_2$, pH 7.2. Free Ca^{2+} in the pipette solution was 205 nM, measured fluorimetrically with fura-2. External solution contained (in mM) 130 NaCl, 5 CsCl, 1.2 $MgSO_4$, 1.2 NaH_2PO_4, 5 $CaCl_2$, 10 HEPES, 10 Na^+ HEPES and 10 glucose, pH 7.4. Verapamil (1 μM) was used to block I_{Ca}. Our measurement conditions were biased towards measuring outward (3 Na^+ out: 1 Ca^{2+} in) I_{NaCa}. (A). After holding the myocyte at the calculated reversal potential (−73 mV) of I_{NaCa} for 5 min. (to minimize fluxes through NCX1 and thus allowed $[Na^+]_i$ and $[Ca^{2+}]_i$ to equilibrate with those in pipette solution), I_{NaCa} (30°C) was measured in WT-sham, WT-TAC and NCX1-TAC myocytes using a descending (from +100 to −120 mV; 500 mV/s) - ascending (from −120 to +100 mV; 500

mV/s) voltage ramp, first in the absence and then in the presence of 1 mM $NiCl_2$. (B). Raw currents measured in a WT-sham myocyte. I_{NaCa} was defined as the difference current measured in the absence and presence of Ni^+ during the descending voltage ramp. Note that with the exception of small contamination of the ascending ramp by the cardiac Na^+ current, there were little to no differences in currents measured between the descending and ascending voltage ramps. This suggests that $[Ca^{2+}]_i$ and $[Na^+]_i$ sensed by NCX1 did not appreciably change by NCX1 fluxes during the brief (880 ms) voltage ramp. I_{NaCa} was divided by C_m prior to comparisons. (C). Current-voltage relationships of I_{NaCa} (means ± SE) from WT-sham (;n=7 myocytes from 4 mice), WT-TAC (◇ n=10 myocytes from 3 mice) and NCX1-TAC (○; n=8 myocytes from 3 mice) myocytes are shown. The reversal potential of I_{NaCa} was ~−60 mV, close to the theoretical reversal potential of −73 mV. Error bars are not shown if they fall within the boundaries of the symbol.

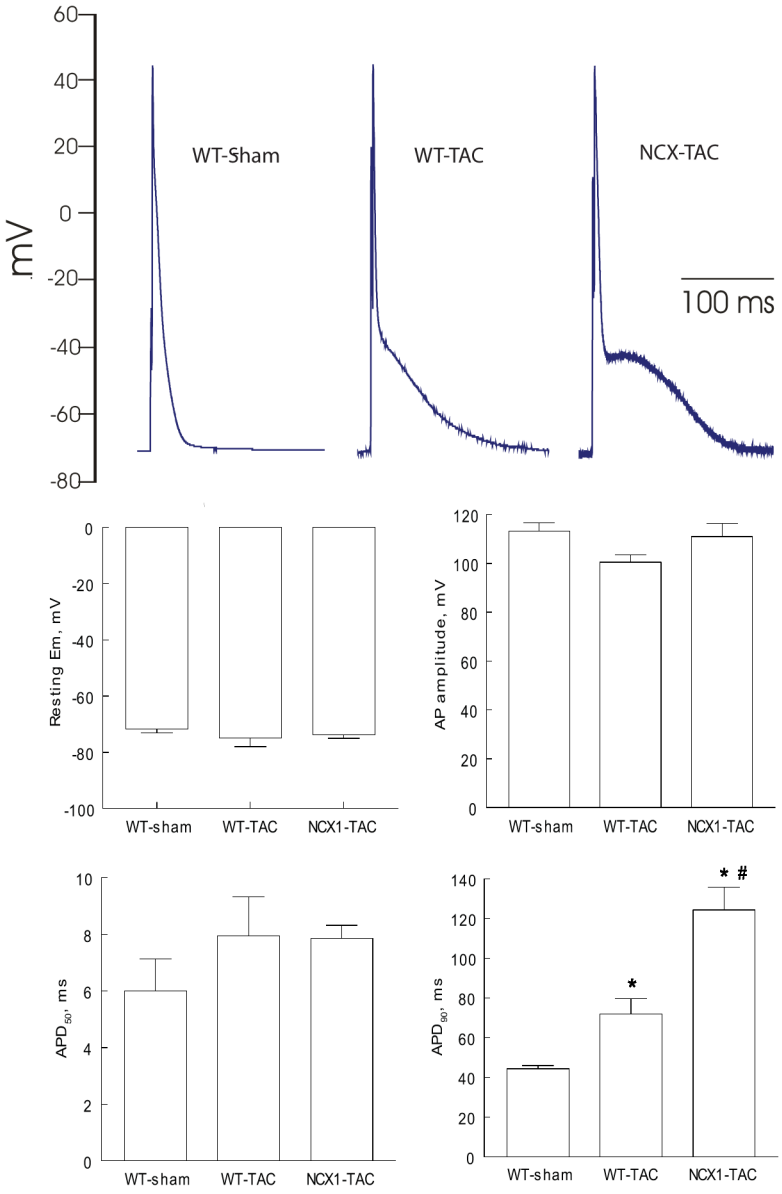

Figure 5. Effects of induced overexpression of Na^+/Ca^{2+} exchanger (NCX1) and transverse aortic constriction (TAC) on action potential (AP)

Myocytes were paced at 1 Hz. Pipette solution consisted of (in mM) 125 KCl, 4 $MgCl_2$, 0.06 $CaCl_2$, 10 HEPES, 5 K^+-EGTA, 3 Na_2ATP, and 5 Na_2-creatine phosphate (pH 7.2). External solution consisted of (in mM) 132 NaCl, 5.4 KCl, 1.8 $CaCl_2$, 1.8 $MgCl_2$, 0.6 NaH_2PO_4, 7.5 HEPES, 7.5 Na^+-HEPES, and 5 glucose, pH 7.4. (A). Representative AP from WT-sham, WT-TAC and NCX1-TAC myocytes recorded using current-clamp configuration at 1.5× threshold stimulus, 4-ms duration and at 30°C (4, 17, 46, 47). (B). Means ± SE of resting membrane potential (E_m), action potential amplitude, action potential duration at 50% (APD_{50}) and at 90% repolarization (APD_{90}) from 14 WT-sham (4 mice), 5 WT-TAC (2 mice) and 10 NCX1-TAC (4 mice) myocytes are shown. * $p<0.0001$, WT-sham vs. WT-TAC or NCX1-TAC; #$p<0.01$, WT-TAC vs. NCX1-TAC.

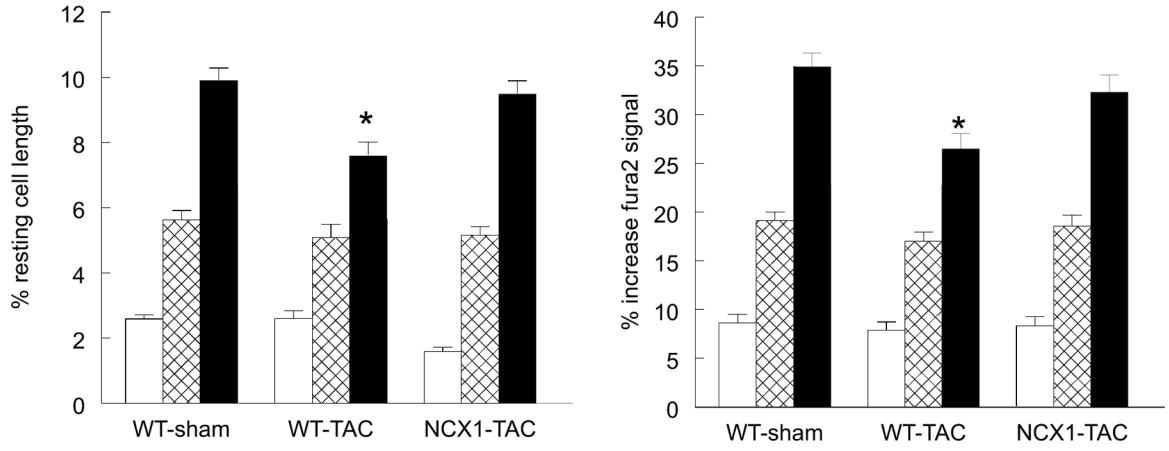

Figure 6. Effects of induced overexpression of Na^+/Ca^{2+} exchanger (NCX1) and transverse aortic constriction (TAC) on myocyte contractility and $[Ca^{2+}]_i$ transient amplitudes

LV myocytes were paced (2 Hz) to contract at 37°C and 0.6 (open), 1.8 (hatched) or 5.0 mM (filled) $[Ca^{2+}]_o$ (Methods). Left: means ± SE of maximal contraction amplitude (% resting cell length) from WT-sham (n=12, 12 and 13 at 0.6, 1.8 and 5.0 mM $[Ca^{2+}]_o$), WT-TAC (n=9, 10 and 12 at 0.6, 1.8 and 5.0 mM $[Ca^{2+}]_o$), and NCX1-TAC (n=15, 21 and 21 at 0.6, 1.8 and 5.0 mM $[Ca^{2+}]_o$) myocytes. Myocytes were isolated from 2 WT-sham, 3 WT-TAC and 3 NCX1-TAC mice. *$p<0.0009$ (group × $[Ca^{2+}]_o$ interaction effect), WT-TAC vs. WT-sham or NCX1-TAC. Right: means ± SE of $[Ca^{2+}]_i$ transient amplitude (% increase fura2 signal) from WT-sham (n=15, 21 and 20 at 0.6, 1.8 and 5.0 mM $[Ca^{2+}]_o$), WT-TAC (n=10, 16 and 17 at 0.6, 1.8 and 5.0 mM $[Ca^{2+}]_o$), and NCX1-TAC (n=14, 12 and 12 at 0.6, 1.8 and 5.0 mM $[Ca^{2+}]_o$) myocytes. Myocytes were isolated from 5 WT-sham, 3 WT-TAC and 3 NCX1-TAC mice. *$p<0.02$ (group × $[Ca^{2+}]_o$ interaction effect), WT-TAC vs. WT-sham or NCX1-TAC. $[Ca^{2+}]_i$ transients results are summarized in Table 1.

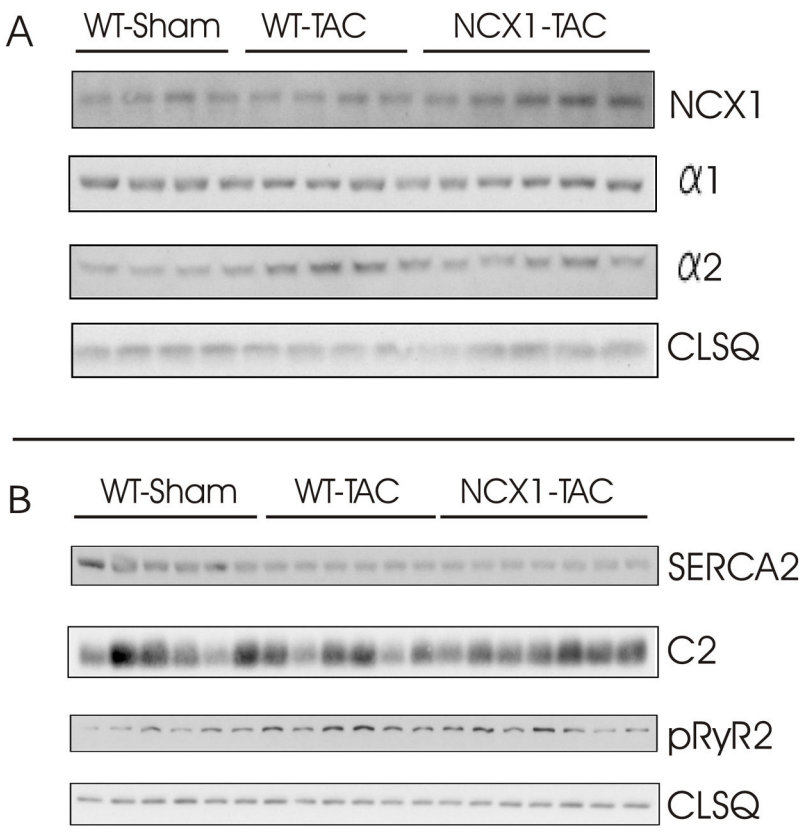

Figure 7. Effects of induced overexpression of Na^+/Ca^{2+} exchanger (NCX1) and transverse aortic constriction (TAC) on the expression of selected proteins involved in excitation-contraction coupling

Crude membranes (Na^+/Ca^{2+} exchanger, α_1- and α_2-subunits of Na^+-K^+-ATPase) or homogenates (SERCA2, ryanodine receptor phosphorylated at serine^{2808}, phospholemman and calsequestrin) were prepared from WT-sham, WT-TAC and NCX1-TAC left ventricles and subjected to SDS-PAGE followed by Western blot analysis. Protein loading was 50 μg/lane. Composite results are presented in Table 2.

Table 1

Effects of TAC ± induced NCX1 transgene expression on $[Ca^{2+}]_i$ transients

$[Ca^{2+}]_o$	WT-sham	WT-TAC	NCX1-TAC
	Systolic $[Ca^{2+}]_i$, nM		
0.6	146 ± 14 (15)	137 ± 12 *(10)	136 ± 9 (14)
1.8	223 ± 14 (21)	191 ± 8 *(16)	199 ± 10 (12)
5.0	337 ± 19 (20)	267 ± 12 *(17)	305 ± 19 (12)
	Diastolic $[Ca^{2+}]_i$, nM		
0.6	100 ± 10	98 ± 9	96 ± 9
1.8	112 ± 8	103 ± 6	102 ± 8
5.0	113 ± 8	113 ± 5	113 ± 11
	$[Ca^{2+}]_i$ transient amplitude, % increase in fura2 signal		
0.6	8.6 ± 0.9	7.9 ± 0.8 *	8.3 ± 0.9#
1.8	19.1 ± 0.9	17.0 ± 0.9 *	18.6 ± 1.1#
5.0	34.9 ± 1.4	26.5 ± 1.6 *	32.3 ± 1.8#
	$t_{1/2}$ of $[Ca^{2+}]_i$ transient decline, ms		
0.6	305 ± 17	290 ± 29 *	272 ± 18#
1.8	208 ± 11	244 ± 16 *	204 ± 10#
5.0	168 ± 8	207 ± 11 *	158 ± 6#

Values are means ± SE. Numbers in parentheses are no. of myocytes, without regard to the number of cells contributed by each heart (n=5, 3 and 3 hearts each for WT-sham, WT-TAC and NCX1-TAC, respectively). $[Ca^{2+}]_O$, extracellular Ca^{2+} concentration; NCX1, cardiac Na^+/Ca^{2+} exchanger; TAC, transverse aortic constriction; WT, wild-type. Data were analyzed by 2-way ANOVA (group, $[Ca^{2+}]_O$).

*$p<0.05$, group × $[Ca^{2+}]_O$ interaction effect; WT-sham vs. WT-TAC.

#$p<0.02$, group or group × $[Ca^{2+}]_O$ interaction effect; WT-TAC vs. NCX1-TAC.

Table 2

Effects of TAC ± induced NCX1 transgene expression on selected proteins

	WT-sham	WT-TAC	NCX1-TAC
Crude membrane preparations			
NCX1	1.17 ± 0.05 (4)	1.64 ± 0.17 * (4)	2.28 ± 0.19 # (5)
α1, Na^+-K^+-ATPase	0.64 ± 0.15	0.86 ± 0.10	0.93 ± 0.06
α2, Na^+-K^+-ATPase	0.11 ± 0.02	0.23 ± 0.03 *	0.11 ± 0.02 #
LV homogenates			
SERCA2	3.20 ± 0.33 (6)	1.69 ± 0.06 * (6)	1.41 ± 0.04 # (7)
Phospholemman	2.17 ± 0.28	2.07 ± 0.13	2.30 ± 0.10
pRyR2	0.47 ± 0.10	1.03 ±0.12 *	0.79 ± 0.14

Values are means ± SE; numbers in parentheses are numbers of hearts used in crude membrane preparations or homogenates. Since the π11–13 antibody signal is 1.7× stronger for endogenous mouse NCX1 compared to rat NCX1 transgene (7), NCX1 signals in NCX1-TAC myocytes have been proportionally corrected. Protein band intensities of each protein are divided by the intensities of their respective calsequestrin loading controls. NCX1, cardiac Na^+/Ca^{2+} exchanger; SERCA2, sarco(endo)plasmic reticulum Ca^{2+}-ATPase; pRyR2, ryanodine receptor phosphorylated at $serine^{2808}$; LV, left ventricle; WT, wild-type; TAC, transverse aortic constriction.

* $p<0.04$, WT-sham vs. WT-TAC;

# $p<0.045$, WT-TAC vs. NCX1-TAC.